a

Primer	Sequence
BT1010 GH95 BamHI F	TTTGGATCCGGATGTATTCATGCGCAGG
BT1010 GH95 XhoI R	AAACTCGAGTTATTTTCCAATCAATATATATTCTTGCC
BT1010 N389A F	CTGTGCTATC**GCT**CTGGAAATGAATTACTGG
BT1010 N389A R	GTATATTTGCTATCCCAGG
BT1010 E516A F	AACTCACCC**GCA**AATGTACATTCC
BT1010 E516A R	GCTTGGGCAGACTACCAA
BT0996 GH137 BamHI F	AAAGGATCCTATGCCCAACGTAAA
BT0996 GH137 XhoI R	AAACTCGAGTTCAGTGATCATCCG
BT0996 E159Q F	GCACCACTCTTTGTCGGACTG
BT0996 E159Q R	TTTTACAGC**TTG**ATAACCTGTACCTTC
BT0996 N227A F	CCGTTTGTGATGTTTTAC**GCT**GCGGGA
BT0996 N227A R	GGCACCCAGTGTTTTGTCTTTATCCCAG
BT0996 E240A F	TTAAAGGGT**GCA**CGGGTA
BT0996 E240A R	ATCAGTTTCCGGATGAC

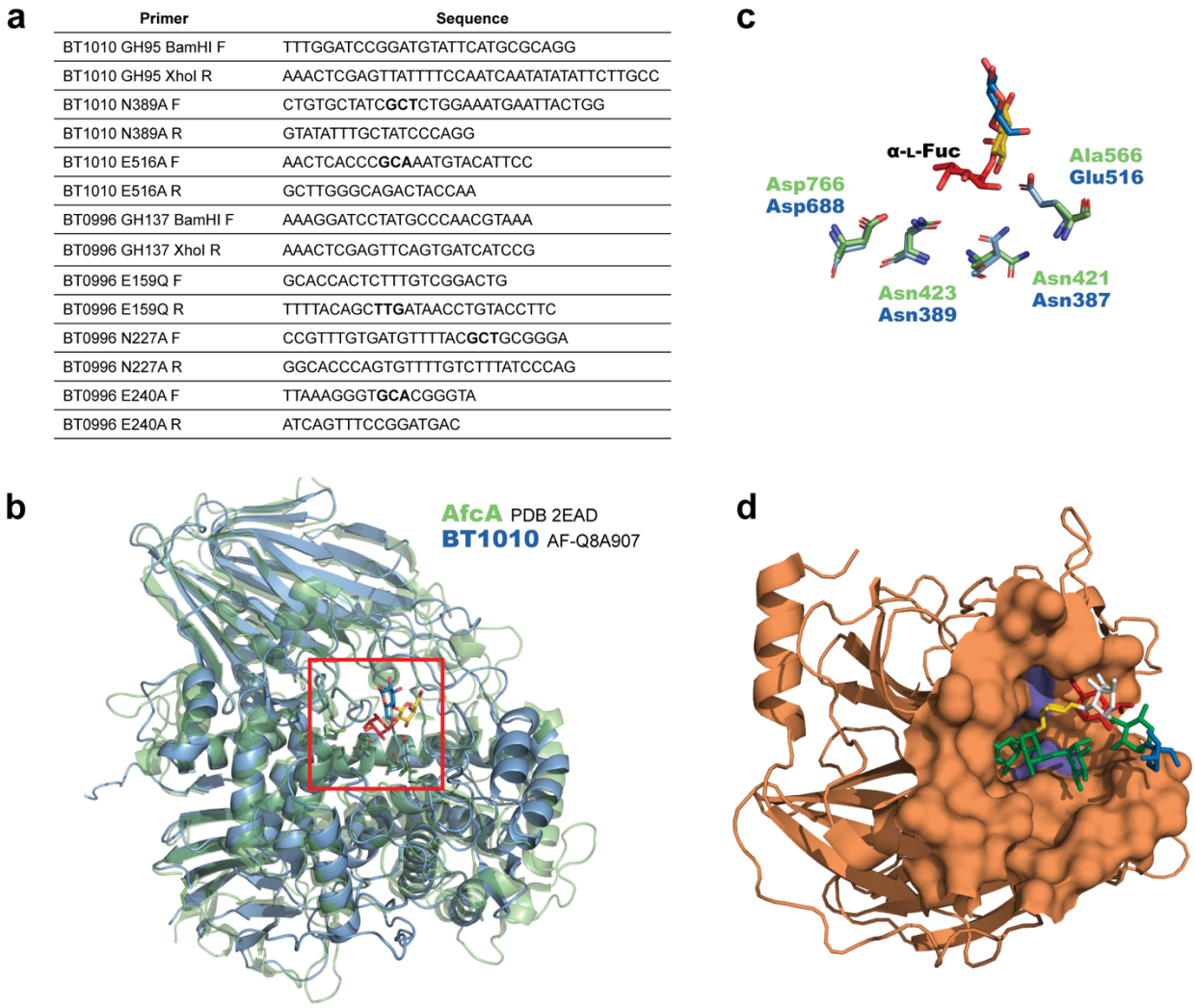

SI Figure 1. Structure guided engineering of BT1010 GH95 and BT0996 GH137 variants
a, Primers used for cloning and mutagenesis of BT1010 GH95 and BT0996 GH137 fusion proteins. **b,** Cartoon overlay of an AlphaFold predictive model of BT1010 GH95 (blue; AF-Q8A907) and the α-L-fucosidase domain of AfcA from *Bifidobacterium bifidum* (green; PDB 2EAD). The red square highlights the active site of the AfcA D766A mutant in complex with 2'-Fucosyllactose (2'-FL). **c,** AfcA catalytic residues (green) that interact with L-Fucose. These residues are conserved within the GH95 family and correspond to Glu516, Asp688, Asn387, and Asn389 in BT1010 (blue). **d,** Cartoon structure of the BT0996 N-terminal GH137 catalytic domain with a surface representation of the Sidechain B substrate binding site.

a

Protein	IPTG	Temperature	Time	Protein Length	Molecular Weight	Isoelectric Point	Extinction Coefficient
BT1010 GH95	0.2 mM	16°C	ON	840 aa	94.165 kDa	6.79	168,275
sfGFP-BT1010 GH95	1 mM	30°C	8 hr	1,066 aa	119.789 kDa	6.45	187,310
mRuby3-BT1010 GH95	0.4 mM	16°C	ON	1,066 aa	119.699 kDa	6.49	195,790
BT0996 GH137	0.2 mM	16°C	ON	406 aa	46.448 kDa	8.07	108,875
sfGFP-BT0996 GH137	0.2 mM	16°C	ON	632 aa	72.072 kDa	6.79	127,910
mRuby3-BT0996 GH137	0.4 mM	16°C	ON	632 aa	71.982 kDa	6.93	136,390

Geneious version 2024.0 created by Biomatters.
Available from https://www.geneious.com

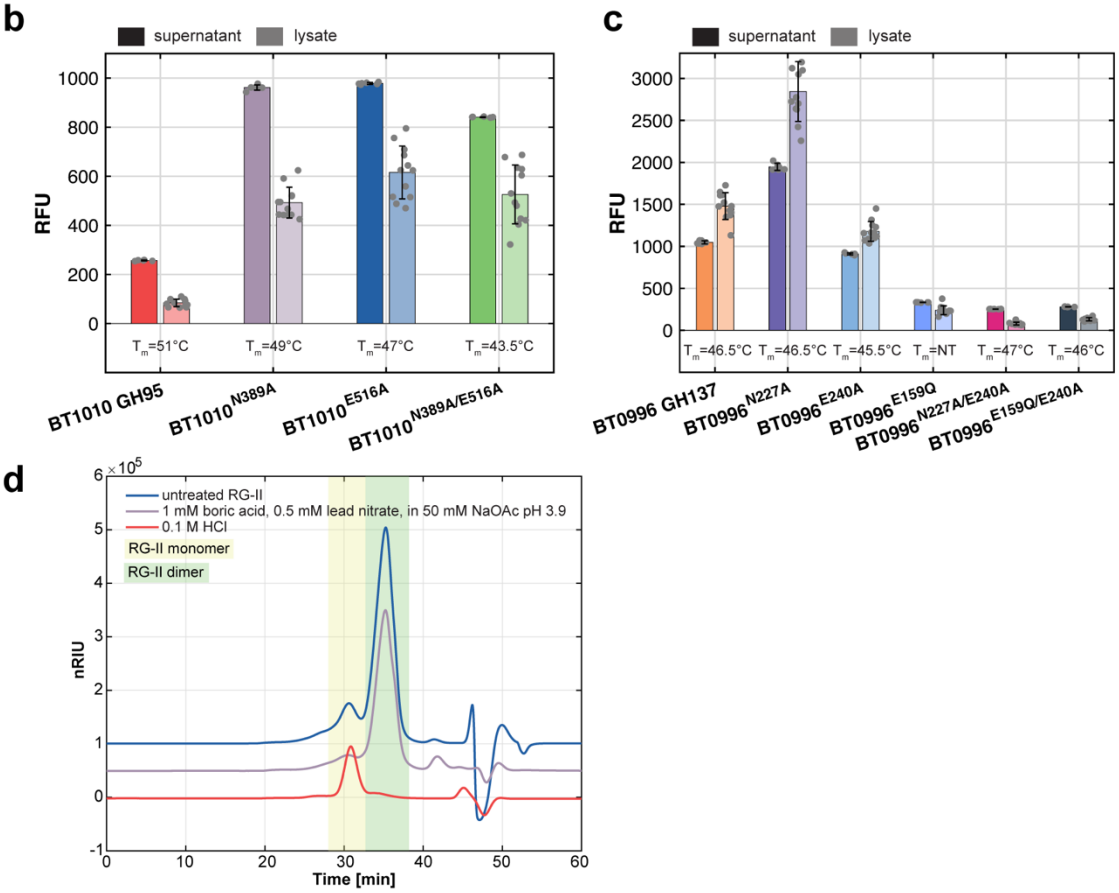

SI Figure 2. Preparation of sfGFP-fusion proteins and RG-II substrates for biochemical characterization
a, Summary of expression conditions and protein information for BT1010 GH95 and BT0996 GH137 fusion proteins. **b,** Expression and thermal stability of native sfGFP-BT1010 and catalytic variants (N389A, E516A, N389A/E516A) or **c,** native sfGFP-BT0996 and catalytic variants (N227A, E240A, E159Q, N227A/E240A, E159Q/E240A). Each bar represents the mean fluorescence of either the expression medium (right, *n*=6) or cell lysate (left, *n*=12) following induction with 0.2 mM IPTG at 16 °C overnight. Overlaid points represent raw data with error bars corresponding to standard deviation. Values below indicate the melting temperature (T_m) derived from thermal shift assays. NT= not tested. **d,** Isolation and characterization of RG-II substrates using size-exclusion chromatography (SEC). Chromatograms show the respective ratio of RG-II monomer (yellow box) and dimer (green box) present before (blue) and after *in vitro* dimerization (purple) or monomerization (red).

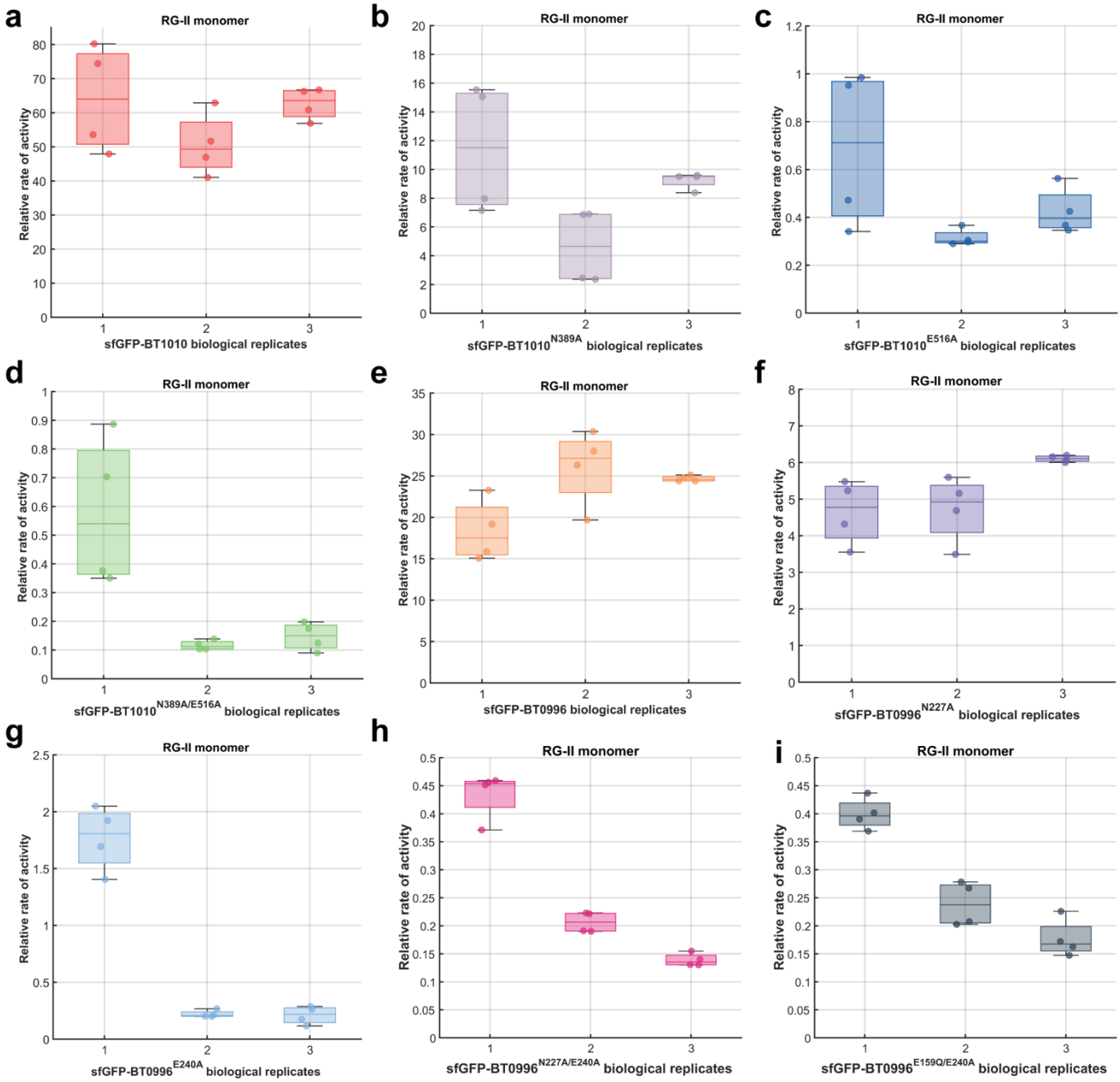

SI Figure 3. Catalytic activity of sfGFP-BT1010 and sfGFP-BT0996 fusion proteins against RG-II monomer
a, Quantification of L-Gal released from 1 mM RG-II monomer by native sfGFP-BT1010 (red) or variants **b,** N389A (purple) **c,** E516A (blue) **d,** double mutant N389A/E516A (green). **e,** Quantification of L-Ara*f* released from 1 mM RG-II monomer by native BT0996 GH137 (orange) or variants **f,** N227A (purple), **g,** E240A (blue), and double mutants **h,** N227A/E240A (magenta) and **i,** E159Q/E240A (navy). The relative rate of activity is calculated from the mass of hydrolyzed product detected in a 25 µL injection volume ($ng \cdot min^{-1} \cdot \mu M^{-1}$). Boxplots represent 3 independent protein expressions and overlaid points indicate 4 independent HPAEC-PAD injections. For each box, the line inside is the sample median while the top and bottom edges are the upper and lower quartiles, respectively. Whiskers extend to maximum and minimum values.

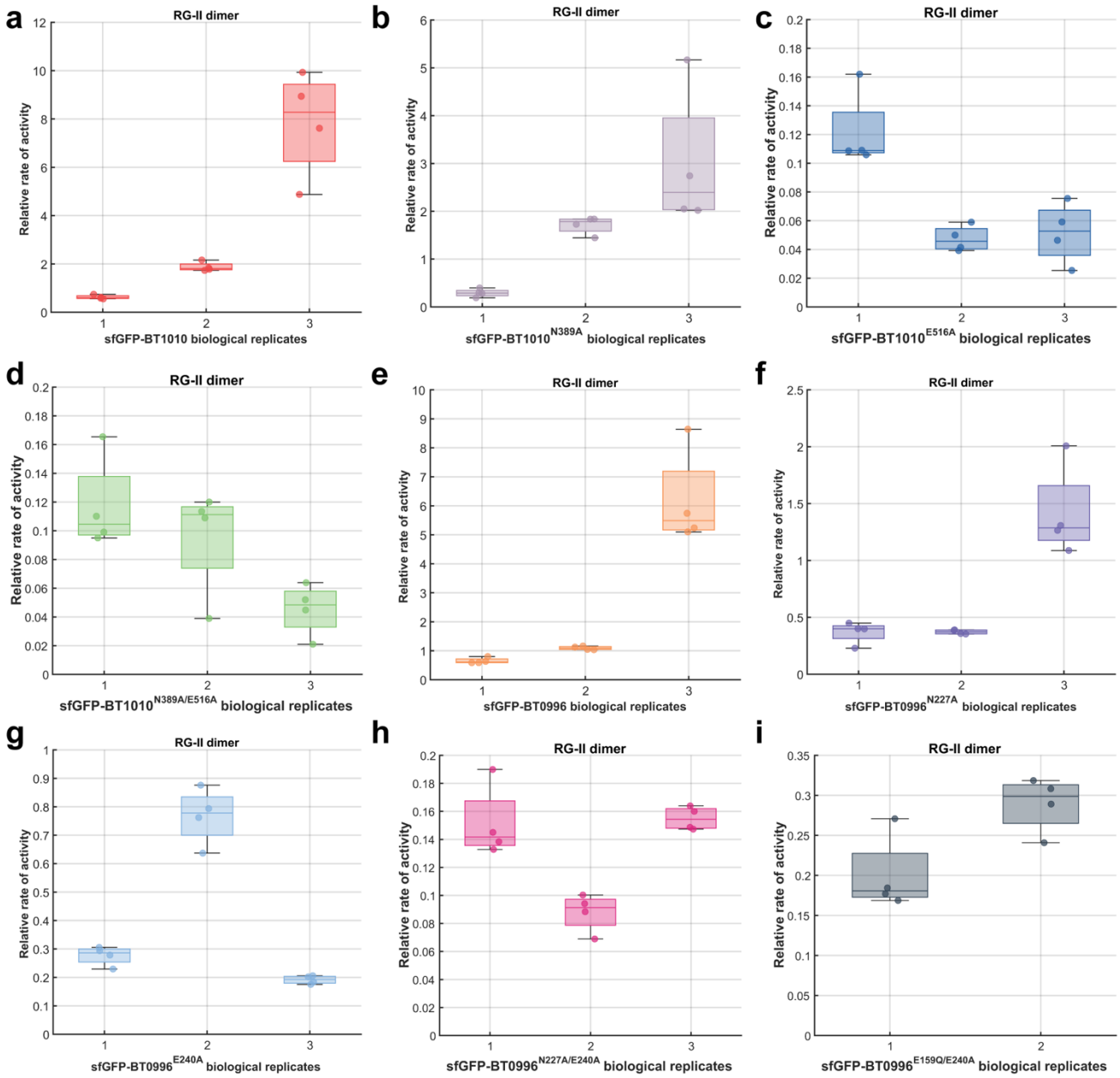

SI Figure 4. Catalytic activity of sfGFP-BT1010 and sfGFP-BT0996 fusion proteins against RG-II dimer
a, Quantification of L-Gal released from 0.5 mM RG-II dimer by native sfGFP-BT1010 or variants **b,** N389A **c,** E516A **d,** double mutant N389A/E516A. **e,** Quantification of L-Ara*f* released from 0.5 mM RG-II dimer by native BT0996 GH137 or variants **f,** N227A **g,** E240A, and double mutants **h,** N227A/E240A and **i,** E159Q/E240A. The relative rate of activity is calculated from the mass of hydrolyzed product detected in a 25 µL injection volume ($ng \cdot min^{-1} \cdot \mu M^{-1}$). Boxplots represent independent protein expression and overlaid points indicate 4 independent HPAEC-PAD injections. For each box, the line inside is the sample median while the top and bottom edges are the upper and lower quartiles, respectively. Whiskers extend to maximum and minimum values.

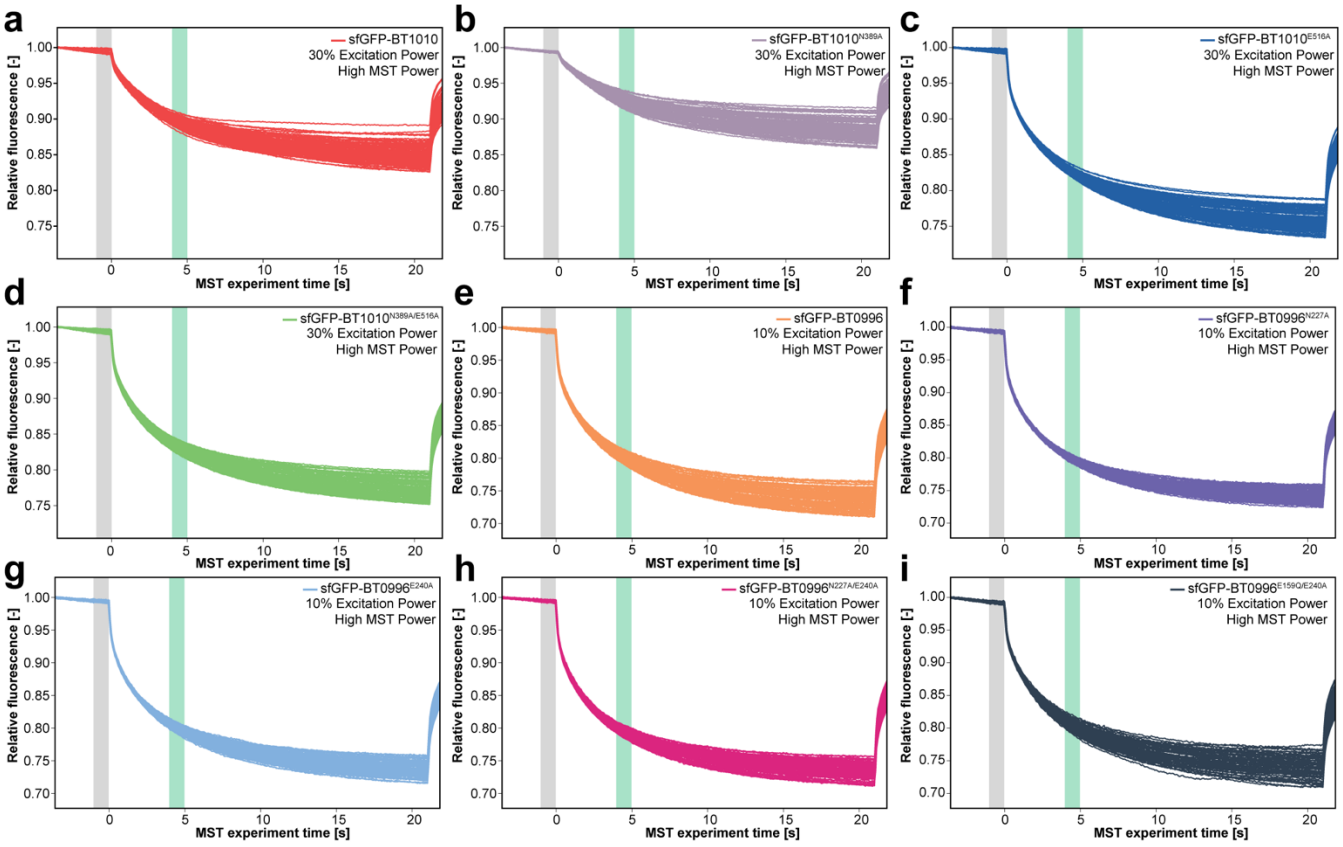

SI Figure 5. Binding analysis between sfGFP-BT1010 and sfGFP-BT0996 fusion proteins and RG-II monomer
a, MST traces for binding between RG-II monomer and native sfGFP-BT1010 (red) or variants **b,** N389A (purple) **c,** E516A (blue) **d,** double mutant N389A/E516A (green). **e,** MST traces for binding between RG-II monomer and native sfGFP-BT0996 (orange) or variants **f,** N227A (purple) **g,** E240A (blue), and double mutants **h,** N227A/E240A (magenta) and **i,** E159Q/E240A (navy). Representative MST traces depict the change in fluorescence intensity of one capillary over time. The green rectangle indicates a MST-on time of 5 sec was used for analysis.

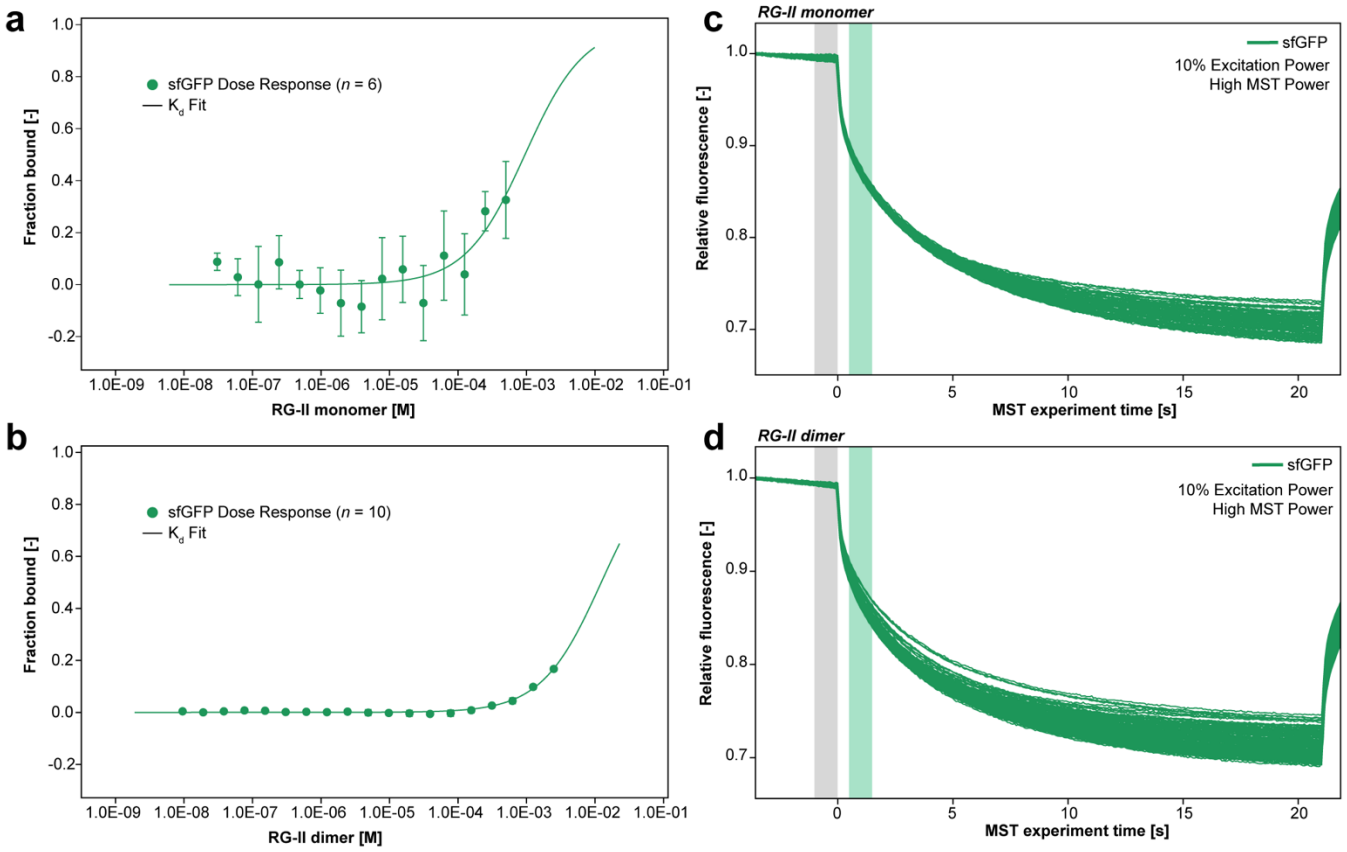

SI Figure 6. Binding analysis between sfGFP and RG-II monomer or dimer
a, Dose-response curves between sfGFP and RG-II monomer were generated from the means of *n* = 6 independently pipetted measurements with error bars representing standard deviation. **b,** Dose-response curves between sfGFP and RG-II dimer were generated from the means of *n* = 10 independently pipetted measurements with error bars representing standard deviation. **c,** MST traces for binding between sfGFP and RG-II monomer or **d,** dimer. Representative MST traces depict the change in fluorescence intensity of one capillary over time. The green rectangle indicates a MST-on time of 1.5 sec was used for analysis.

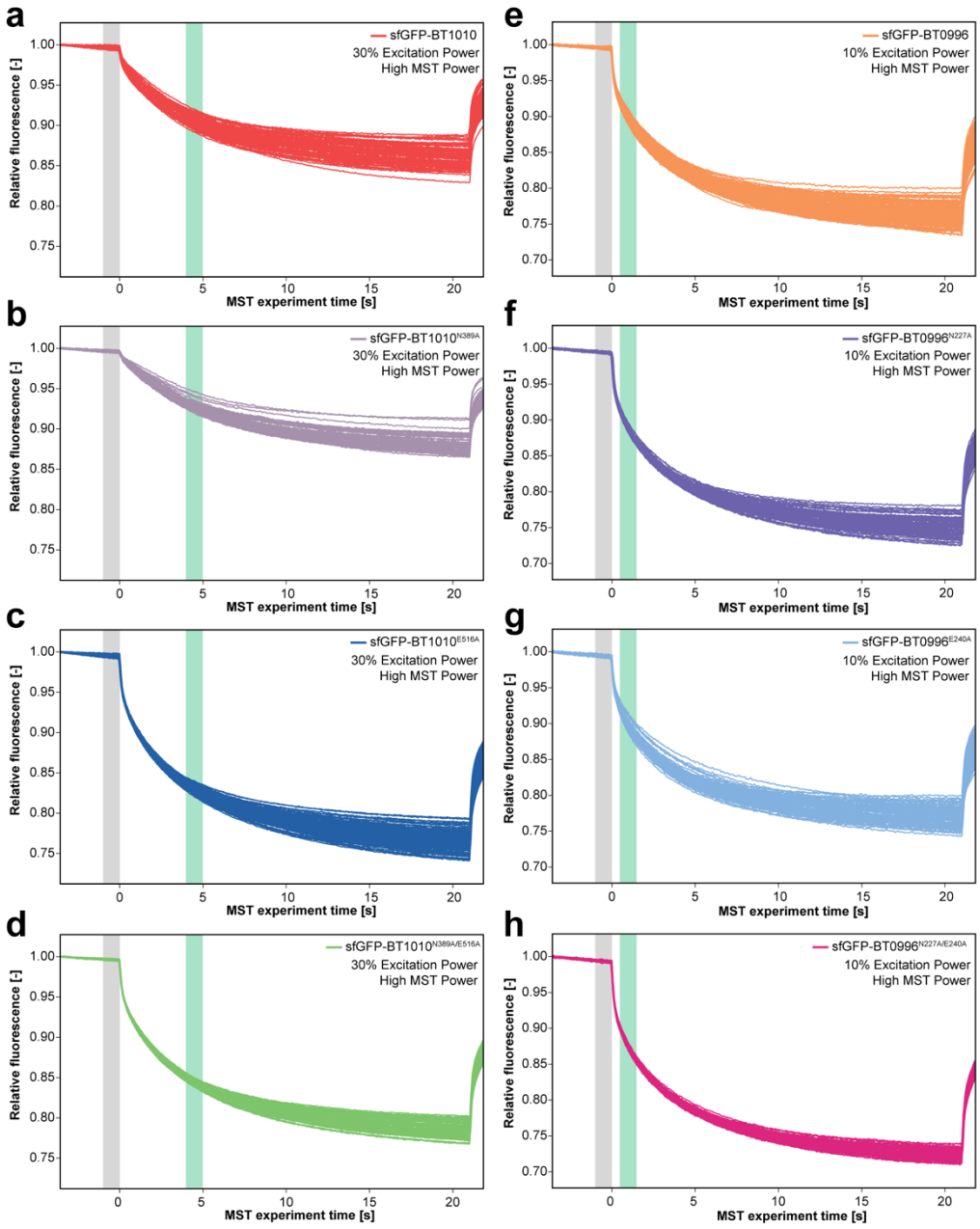

SI Figure 7. Binding analysis between sfGFP-BT1010 and sfGFP-BT0996 fusion proteins and RG-II dimer
a, MST traces for binding between RG-II dimer and native sfGFP-BT1010 or variants **b,** N389A **c,** E516A **d,** double mutant N389A/E516A. **e,** MST traces for binding between RG-II dimer and native sfGFP-BT0996 or variants **f,** N227A **g,** E240A, and double mutant **h,** N227A/E240A. Representative MST traces depict the change in fluorescence intensity of one capillary over time. The green rectangle indicates the MST-on time used for analysis.

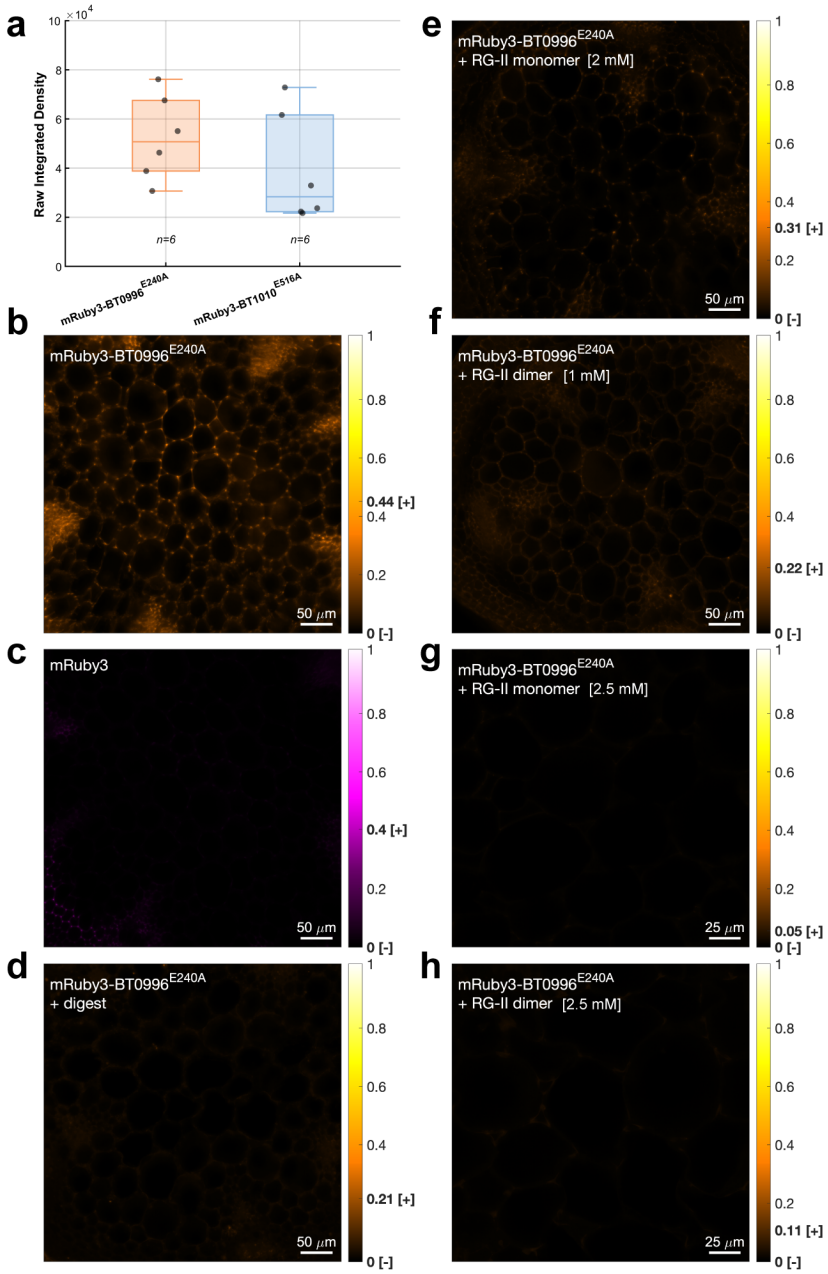

SI Figure 8. Fluorescent labeling of *Arabidopsis thaliana* stem sections
a, Comparison of fluorescence intensities between mRuby3-BT0996^{E240A} and mRuby3-BT1010^{E516A}. Boxplots represent raw integrated densities, where the inner line is the sample median while the top and bottom edges are the upper and lower quartiles, respectively. Whiskers extend to maximum and minimum values. Overlaid points indicate values from *n* = 6 independent images. **b,** Maximum projection images of sections labeled with 0.4 μM mRuby3-BT0996^{E240A}, **c,** 0.4 μM mRuby3, **d,** 0.4 μM mRuby3-BT0996^{E240A} after pretreatment with 1 μM native BT0996 GH137, **e,** 0.4 μM mRuby3-BT0996^{E240A} after preincubation with 2 mM RG-II monomer or **f,** 1 mM RG-II dimer. Scale bars = 50 μm. **g,** 0.4 μM mRuby3-BT0996^{E240A} after preincubation with 2.5 mM RG-II monomer or **h,** 2.5 mM RG-II dimer. Scale bars = 25 μm. Color scales indicate the normalized maximum [+] and minimum [-] pixel intensities in each image.

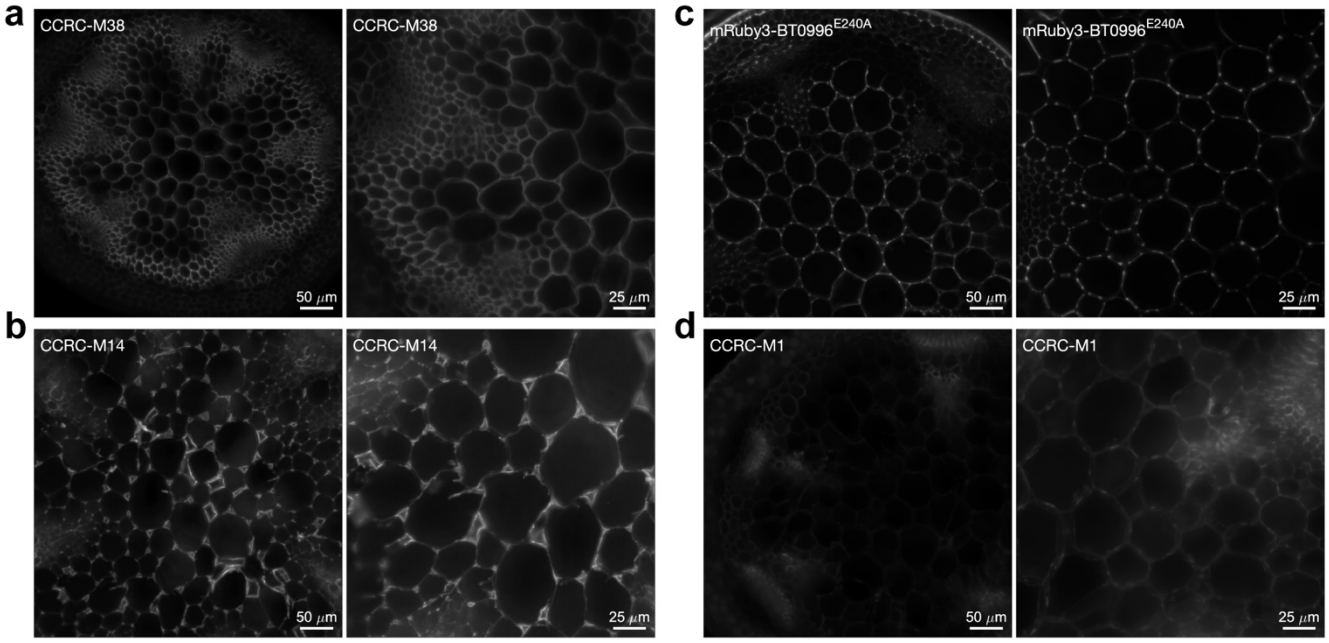

SI Figure 9. Distinct labeling of *Arabidopsis thaliana* stem sections with mRuby3-BT0996^{E240A} and plant glycan-directed monoclonal antibodies

a, Fluorescence images (left – 10X, right – 20X) showing labeling with CCRC-M38 (de-esterified HG), **b**, CCRC-M14 (RG-I backbone), **c**, mRuby3–BT0996^{E240A} (RG-II), or **d**, CCRC-M1 (fucosylated xyloglucan). 10X scale bars = 50 μm, 20X scale bars = 25 μm. All images are maximum projection images generated from z-stacks.

Figure	Comparison	Test type	Test statistics
2C	Native vs variant BT1010 GH95 against RG-II monomer	One-way ANOVA	F(3,8) = 144.31, *P*-value = 2.65E-07
	Native vs variant BT1010 GH95 against RG-II dimer	One-way ANOVA	F(3,8) = 1.868, *P*-value = 0.213
3C	Native vs variant BT0996 GH137 against RG-II monomer	One-way ANOVA	F(4,10) = 77.99, *P*-value = 1.69E-07
	Native vs variant BT0996 GH137 against RG-II dimer	One-way ANOVA	F(4,9) = 1.425, *P*-value = 0.302
2D	Native BT1010 GH95 against RG-II monomer vs dimer	Paired t-test, Bonferroni-Holm correction	t(2) = 13.101, *P*-value (raw) = 0.006, *P*-value (corrected) = 0.023
	BT1010^{N389A} against RG-II monomer vs dimer	Paired t-test, Bonferroni-Holm correction	t(2) = 2.841, *P*-value (raw) = 0.105, *P*-value (corrected) = 0.209
	BT1010^{E516A} against RG-II monomer vs dimer	Paired t-test, Bonferroni-Holm correction	t(2) = 6.566, *P*-value (raw) = 0.022, *P*-value (corrected) = 0.067
	BT1010$^{N389A/E516A}$ against RG-II monomer vs dimer	Paired t-test, Bonferroni-Holm correction	t(2) = 1.438, *P*-value (raw) = 0.287, *P*-value (corrected) = 0.287
3D	Native BT0996 GH137 against RG-II monomer vs dimer	Paired t-test, Bonferroni-Holm correction	t(2) = 8.820, *P*-value (raw) = 0.013, *P*-value (corrected) = 0.05
3D	BT0996^{N227A} against RG-II monomer vs dimer	Paired t-test, Bonferroni-Holm correction	t(2) = 35.397, *P*-value (raw) = 0.0008, *P*-value (corrected) = 0.004
	BT0996^{E240A} against RG-II monomer vs dimer	Paired t-test, Bonferroni-Holm correction	t(2) = 0.528, *P*-value (raw) = 0.650, *P*-value (corrected) = 1.30
	BT0996$^{N227A/E240A}$ against RG-II monomer vs dimer	Paired t-test, Bonferroni-Holm correction	t(2) = 1.486, *P*-value (raw) = 0.276, *P*-value (corrected) = 0.8268
	BT0996$^{E159Q/E240A}$ against RG-II monomer vs dimer	Paired t-test, Bonferroni-Holm correction	t(1) = 0.597, *P*-value (raw) = 0.657, *P*-value (corrected) = 1.30
6F	Fluorescence intensity of mRuby3–BT0996^{E240A} vs controls	Linear mixed-effects model	F(4,86) = 57.74, *P*-value = 1.41E-23
	mRuby3–BT0996^{E240A} vs mRuby3	F-test on fixed effect contrast with Bonferroni correction	F(1,86) = 120.89, *P*-value (raw) = 4.49E-18, *P*-value (corrected) = 2.25E-17
	mRuby3–BT0996^{E240A} vs BT0996 digest	F-test on fixed effect contrast with Bonferroni correction	F(1,86) = 94.85, *P*-value (raw) = 1.54E-15, *P*-value (corrected) = 7.71E-15
	mRuby3–BT0996^{E240A} vs RG-II monomer	F-test on fixed effect contrast with Bonferroni correction	F(1,86) = 88.01, *P*-value (raw) = 8.24E-15, *P*-value (corrected) = 4.12E-14
	mRuby3–BT0996^{E240A} vs RG-II dimer	F-test on fixed effect contrast with Bonferroni correction	F(1,86) = 9.05, *P*-value (raw) = 0.003, *P*-value (corrected) = 0.017
	RG-II monomer vs RG-II dimer	F-test on fixed effect contrast with Bonferroni correction	F(1,86) = 71.49, *P*-value (raw) = 6.32E-13, *P*-value (corrected) = 3.16E-12

SI Table 1. Summary of statistical analyses